Full-Speed Testing of Silicon Photonic Electro-Optic Modulators from Picowatt-level Scattered Light

Xiaoxi Wang^{1,*}, Boris A. Korzh², Matthew D. Shaw², and Shayan Mookherjea^{1,*}

¹ University of California, San Diego, Electrical & Computer Engineering, La Jolla, CA 92093-0407, USA
² Jet Propulsion Laboratory, California Institute of Technology, 4800 Oak Grove Drive, Pasadena, CA 91109, USA
*E-mail: xiw270@ucsd.edu, smookherjea@ucsd.edu

Abstract: We demonstrate a technique for measuring the full-speed performance of integrated modulators from ultraweak surface-coupled and scattered light. This can enable rapid characterization of unpackaged, high-speed wafer-scale integrated photonics without test ports or special fabrication. © 2020 The Author(s)

1. Introduction. A modern silicon photonic wafer may contain hundreds or thousands of high-speed electro-optic devices, such as Mach-Zehnder modulators (MZM), electro-absorption modulators, switches, phased-array structures etc. [1,2]. Devices operated near their performance limits routinely show variability in precise RF-optical index matching or in the termination impedance, as well as low extinction ratio, which makes their high-frequency behavior not predictable from DC or low-frequency measurements alone. Singulating wafers into dies and performing careful fiber alignment on each device that is necessary in order to collect enough light to measure high-speed eye diagrams, for example, is among the most slow and costly processes in integrated photonics manufacturing [1,3,4]. Optical input/output test ports (e.g., couplers, tap power splitters, metal probing pads etc.) may be fabricated, but their inclusion leads to increased loss, added noise and poor scaling, and sometimes, added fabrication complexity [5-7]. Alternative methods for stand-off testing include fabricating metal pads onto the optical circuit, or metal gratings fabricated onto fiber probe facets, but have only yielded DC or low frequency (sub-MHz) data, even when in contact with the waveguide [8,9].

Here, we demonstrate stand-off measurement of the full-speed operation of fully-fabricated photonic integrated MZM's without dedicated test ports, grating couplers, near-field coupling, or any special fabricated features. No grating couplers or special waveguide features were fabricated in the silicon photonic wafer, and the devices have ~ 4 µm of unplanarized, top-cladding oxides. MZM's were operated close to their limits, with limited extinction ratio, presenting practical challenges for low-noise, high-fidelity oscilloscopic capture. Our measurement technique successfully uses the ultra-weak (picowatts or less) of optical power that is obtained when simply shining light from a milliwatt-class continuous-wave diode laser loosely onto the feeder waveguide, modulating the device electrodes with an RF test pattern and capturing the scattered, modulated light from a waveguide segment for detection. Eye diagrams are acquired and analyzed at optical power levels 80 dB lower than necessary for a conventional optical sampling oscilloscope (Keysight, Tektronix etc.). Clear discrimination is obtained of the modulated test signal against the unmodulated background detection events, which can assist in rapid alignment and high-throughput testing. While final-stage testing and qualification will still be done after assembly, such measurements as shown here can help both early-stage high-speed diagnostics and guide further processing.

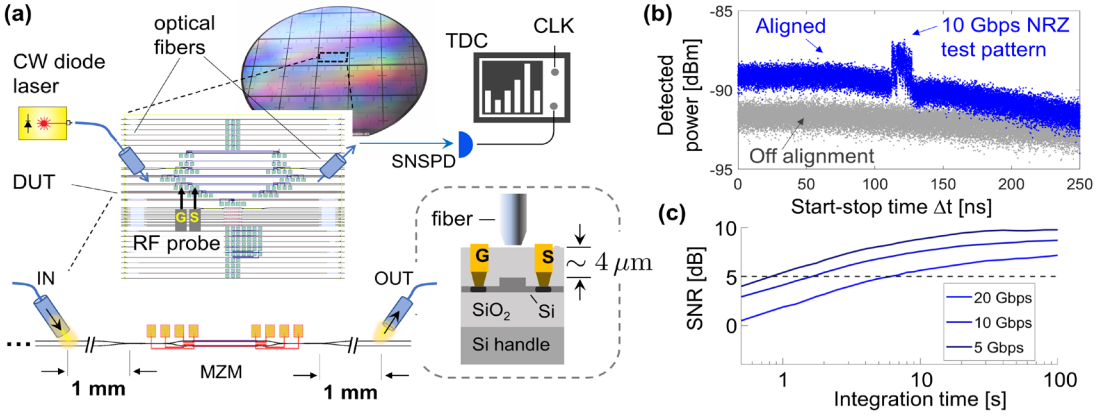


Fig. 1(a). Working principle: Collecting weakly waveguide-coupled and -scattered light after modulation by an integrated Mach-Zehnder modulator (MZM) device under test (DUT) which was driven by RF test patterns. Detection using a superconducting nanowire single-photon detector (SNSPD) is performed in the ultra-low power regime. Histograms of the start (photon detection) to stop (clock reference) time difference Δt_n , performed, e.g., by a time-to-digital converter (TDC), reproduces the test RF waveform, over a few seconds. **(b)** Example histogram showing the test pattern above the background light. **(c)** A signal-to-noise ratio calculated from the histogram can identify alignment [e.g., SNR^(align) > 5 dB] rapidly, while the RF probe applies various test patterns to the DUT. The bandwidth limitations of this scheme were also studied.

Th4A.7.pdf OFC 2020 © OSA 2020

2. Experiment. Low- $V\pi$ depletion-mode p-n junction MZM's were fabricated in a foundry process on silicon-oninsulator (SOI) wafers similar to Ref. [10]. Each reticle contains several MZM's and other photonic devices. To permit comparison with conventional edge taper measurement, the device under test (DUT) was singulated from the wafer, but this is not required for routine operation. RF modulation signals generated by an Arbitrary Waveform Generator (AWG70002B, Tektronix) were applied to the DUT using an SG probe landed on the electrical pads. As usual, the MZM has some lengths of input and output single-mode waveguides (0.5 µm width) in the silicon plane. Two fibers were positioned above the chip, i.e., above the un-planarized upper SiO₂ cladding using micrometercontrolled positioning stages at an angle of 40° (input side) and 53° (output side) to the vertical, about 1 mm away from the MZM. Optimal angles depend on the structure, but once determined, remain constant when scanning the same design across a wafer. The input fiber was placed to illuminate a segment of waveguide before the MZM, and the other fiber was placed above a segment of waveguide after the MZM to collect scattered light for detection. A few different fibers available in the laboratory were used, and results are shown when an SMF-28e fiber with a fiber Bragg grating near the cleaved tip was used on the illumination/input side (the recoated jacket was mechanically stripped), and a lensed, tapered fiber (spot size 2.5 µm) was used for the collection/output side. Continuous-wave light at about 1.55 µm wavelength from a fiber-coupled laser diode was used for measurement. The fraction of (unmodulated) light that is coupled into the guided mode of the waveguide from the first fiber is weak, as also is the fraction of scattered light from the waveguide after modulation that is coupled into the output fiber. From an input power of about 20 mW, about 5 pW of average power was coupled to the detector. Detection was performed using a fiber-coupled superconducting nanowire single-photon detector (SNSPD, detection efficiency ~50% at 1550 nm) operated in a cold cryostat at 0.8K. Each photon detected by the SNSPD generated a "start" pulse for a time-todigital converter (TDC) instrument (quTAG, qutools GmbH). A periodic electrical clock (limited to 25 MHz) was sent to one of the electrical inputs of the TDC and generated the trigger of the "stop" signal. The histogram of the start-stop time difference Δt_n , acquired repeatedly (n=1,2, ... enumerates the clock pulses) accurately reproduces the RF waveform that was applied to the DUT, as explained elsewhere [11,12]. At the TDC's maximum clock rate (25 MHz), up to 10 million photons can be processed per second, since less than one detection event should occur per clock tick. There are 40,000 [=(25 MHz)⁻¹(1 ps)⁻¹] time bins accumulating at ~250 events per second, on average. Unmodulated light also finds its way into the output fiber; the start-stop histogram of such events forms a broad, nearly-flat background, with the modulated DUT response above this background.

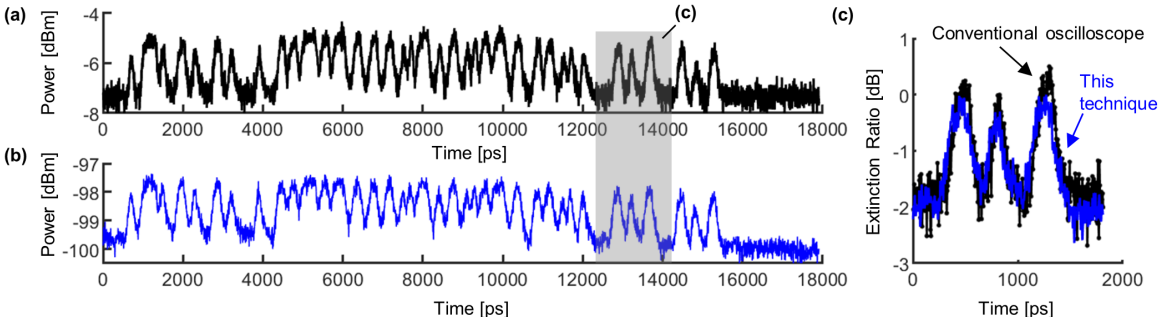


Fig. 2(a) When driving a low- $V\pi$ silicon photonic MZM at 10 Gbit.s⁻¹ close to its known limit [10], a Keysight DCA-X oscilloscope with 86105 module was used to capture an NRZ-encoded pattern, at -6 dBm average power at the receiver front-end. This measurement was performed using traditional edge coupling of waveguides to fibers. (b) The same pattern was detected using the scattering-based scheme [Fig. 1] (c) Magnified view of a short section of panels (a) and (b), showing the agreement, despite the >90 dB difference in detected optical power.

3. Results. (A) Rapid Alignment: Fiber positioning above a device is performed coarsely by visual (camera) guidance, and more accurately by scanning the micropositioning stage when measuring an appropriately-defined signal-to-noise ratio (SNR) metric. When the input and output fibers do not interrogate the waveguides of the RF-modulated MZM, the start-stop histogram $\{\Delta t_n\}$ of collected photons is more or less flat and featureless [see Fig. 1(b), gray trace]. This is because attenuated unmodulated laser light has Poisson statistics, with uniform and identically-distributed inter-arrival times. Once the chip is positioned such that some light couples into and out of the guided mode of the MZM, the test pattern is evident above the background [see Fig. 1(b), blue trace]. As a guide to alignment, we define SNR^(align) as the ratio of the mean signal trace over twice the standard deviation of the background trace. Fig. 1(c) shows SNR for various acquisition times, with 10 ps TDC bin width and different NRZ modulation speeds applied to the DUT. In order to achieve SNR>5 dB, acquisition over just a few seconds is seen to be adequate. Thus, a DUT can be rapidly placed under the fibers by scanning its position for optimal SNR^(align).

(B) High-frequency digital and analog pattern capture: Shown in Fig. 2(b) is the waveform acquired when the MZM was modulated with an NRZ bit sequence. Since the modulators on this wafer lacked RF coplanar

Th4A.7.pdf OFC 2020 © OSA 2020

transmission lines, they were bandwidth limited to about 10 Gbit.s⁻¹ [10] and thus provide a useful test of silicon MZM performance close to the limits with limited extinction ratio and other imperfections. The detected average power was 0.16 pW, the acquisition time was 30 seconds, and the acquired histogram was digitally low-pass filtered with a 50 GHz cutoff. For accurate comparison, Fig. 2(a) also shows the same pattern captured in a conventional way on a singulated chip using waveguide-fiber edge-couplers, and detected using an optical oscilloscope (Keysight DCA-X with 86105 module). The magnified view of a few bits [see Fig. 2(c)] shows the agreement of the waveforms, despite the greater-than-90 dB difference in the power level and low extinction ratio (ER) of the MZM.

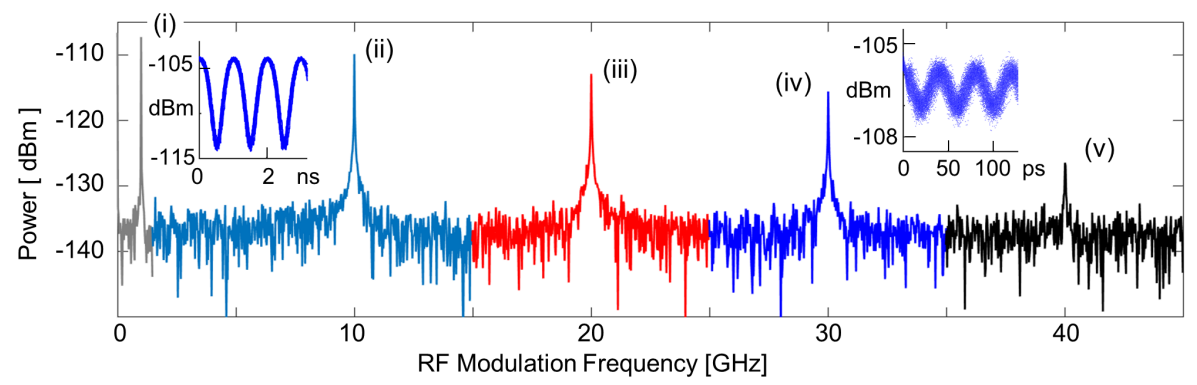


Fig. 3. Optical spectrum analysis. Measurements of RF sinusoidal modulation of a test MZM (with edge couplers) were acquired over 30s using start-stop detection at ultra-low optical power. Each trace was Fourier transformed, resulting in a spectral resolution of 25 MHz. Shown is a composite plot of the main resonances (excluding harmonics) at RF frequencies of (i) 1 GHz [with a short segment of the acquired time-domain 1 GHz modulated optical waveform shown in the inset] (ii) 10 GHz, (iii) 20 GHz, (iv) 30 GHz [with time-domain inset] and (v) 40 GHz.

4. Discussion. Since the random selection of single photons from attenuated laser light (with Poisson statistics) itself results in a Poisson process, the entire test waveform is fair-sampled by the single photon detector, and the histogram faithfully reproduces the test pattern. In contrast to traditional oscilloscopy, scattered light can be rejected in data processing, since it leads to a broad, feature-less distribution of start-stop histogram events, qualitatively different from the test pattern. The key advantage of this technique is that modulation can be quickly detected at five orders of magnitude lower optical power than the so-called quantum limit, $P=2.h.(c/\lambda).B=-50$ dBm for Nyquist bandwidth B=50 GHz [13]. The measurement method described here does not require detection and digitization bandwidths at twice the highest test modulation frequency, which, for high-speed testing, usually requires challenging scan synchronization and calibration methods, and costly cables. Here, the detector requires only simple RF cables, connectors and amplifiers that support only modest RF bandwidth (<1.5 GHz).

Fig. 3 shows the application of this instrumentation as a spectrum analyzer, obtained by taking the Fourier transform of the time trace. A reference MZM on a chip with waveguide-fiber edge couplers was used to capture test sine frequencies past 40 GHz (approximately, the inverse of the measured SNSPD timing jitter, 24 ps) with 30s acquisition time. Even with reduced ER at higher frequencies, we can identify electro-optic modulation up to 40 GHz in the current apparatus at ultralow optical power levels. Certain SNSPD's can support 100 GHz bandwidth pattern capture [12,14], but with low detection efficiency, making them unsuitable at present for testing large numbers of unpackaged, unstabilized modulators rapidly, than the detector used here is able to achieve.

5. Conclusion. Full-speed measurements of integrated Mach-Zehnder modulators is demonstrated at extremely low (<5 picowatts) average optical power, with an acquisition time of a few tens of seconds. Unlike any other technique, such ultra-low power levels are adequate for testing at tens-of-GHz-bandwidth, and thus we may simply shine light onto a feeder waveguide and collect scattered light after the DUT. Rapidly acquiring detailed knowledge of the actual performance of each high-speed device in a wafer without access ports or test structures, and to do so at full operational speed will benefit integrated photonics technology by improving yield and driving down costs.

This work was partially supported by the NSF (CNS-1525090, EFMA-1640968) and NASA (NNX16AD14G, and the Space Technology Research Fellowship, 80NSSC17K0166), and the DARPA Defense Sciences Office, through the DETECT program. Part of the research was performed at the Jet Propulsion Laboratory, California Institute of Technology, under contract with NASA.

6. References. [1] D. Goodwill OFC 2017, M2B.2 [2] C. V. Poulton et al. IEEE J. Sel. Topics Quantum Electron., Vol. 25(5), 7700108 (2019). [3] J. De Coster et al. 21st IEEE European Test Symposium (ETS), Amsterdam, 23-27 May 2016. [4] R. Polster et al. SPIE 10537, Silicon Photonics XIII; 1053703 (2018) [5] D. Vermeulen, L. Chen and C. Doerr. US Patent 10,535,571 (2013) [6] J. R. Ong, et al. OFC 2018, Th2A.11 [7] M. Carminati et al. J. Lightwave Technol. 35(14), 3042 (2017) [8] S. Scheerlink et al. Appl. Phys. Lett. 92(3), 031104 (2008) [9] R. Topley et al. J. Lightwave Technol. 32(12), 2248 (2014) [10] M. R. Watts et al. IEEE J. Sel. Topics Quantum Electron., 16(1), 159 (2010) [11] H. Fedder et al, ECOC 2018, Berlin, (2018) [12] X. Wang, et al. OFC 2019, Th4C.1 [13] D. Marcuse, Principles of Quantum Electronics (Academic Press, New York, 1980). [14] X. Wang et al. J. Lightwave Technol. 38, 166 (2020).